

Journal Pre-proofs

Regular paper

Double-Layered Metamaterial Resonator Operating At Millimetre Wave FOR Detection Of Dengue Virus

Suhail Asghar Qureshi, Zuhairiah Zainal Abidin, Huda A. Majid, Adel YI Ashyap, Chan Hwang See

PII: S1434-8411(22)00031-0
DOI: <https://doi.org/10.1016/j.aeue.2022.154134>
Reference: AEUE 154134

To appear in: *International Journal of Electronics and Communications*

Received Date: 5 October 2021
Revised Date: 26 December 2021
Accepted Date: 22 January 2022

Please cite this article as: S. Asghar Qureshi, Z. Zainal Abidin, H.A. Majid, A. YI Ashyap, C. Hwang See, Double-Layered Metamaterial Resonator Operating At Millimetre Wave FOR Detection Of Dengue Virus, *International Journal of Electronics and Communications* (2022), doi: <https://doi.org/10.1016/j.aeue.2022.154134>

This is a PDF file of an article that has undergone enhancements after acceptance, such as the addition of a cover page and metadata, and formatting for readability, but it is not yet the definitive version of record. This version will undergo additional copyediting, typesetting and review before it is published in its final form, but we are providing this version to give early visibility of the article. Please note that, during the production process, errors may be discovered which could affect the content, and all legal disclaimers that apply to the journal pertain.

© 2022 Published by Elsevier GmbH.



**DOUBLE-LAYERED METAMATERIAL RESONATOR OPERATING AT
MILLIMETRE WAVE FOR DETECTION OF DENGUE VIRUS**

**Suhail Asghar Qureshi¹, Zuhairiah Zainal Abidin^{1*}, Huda A. Majid¹, Adel YI Ashyap²,
Chan Hwang See³**

¹Advanced Telecommunication Research Center (ATRC), Faculty of Electrical and Electronic Engineering, Universiti Tun Hussein Onn Malaysia (UTHM), Batu Pahat, 86400, Johor, Malaysia.

²Center for Applied Electromagnetic (EMCenter), Faculty of Electrical and Electronic Engineering, Universiti Tun Hussein Onn Malaysia (UTHM), Batu Pahat 86400, Johor, Malaysia.

³School of Engineering and the Built Environment, Edinburgh Napier University, Edinburgh EH10 5DT, U.K.

*Corresponding Author: Zuhairiah Zainal Abidin. Email: zuhairia@uthm.edu.my

Abstract

In this paper, a metamaterial-based resonator is proposed for the detection of dengue infection. The replaceable top layer can measure the dielectric characteristics of blood samples to detect the dengue virus. The sensor observed a shift in the resonant frequency towards higher frequencies with the reduction in the blood's permittivity. The sensor showed a 0.325 GHz shift in resonance per unit change in the dielectric permittivity. To corroborate the sensor's practical sensing capability, a sensor prototype was fabricated and validated with alcohol-aqueous solutions. The sensor exhibited shifting of resonance towards lower frequencies with the addition of water contents in methylated alcohol. With the enhanced sensitivity and repeatable measuring capability, the results suggested that this sensor can be applied with real-time

applications on the Internet of Medical Things (IoMT) for early remote detection of the dengue outbreak.

Keywords - Metamaterial, resonator, sensor, millimetre-wave, dengue, IoMT.

1. Introduction

Dengue is a deadly mosquito-borne virus spreading throughout the world. In the last five decades, the prevalence of the dengue virus has climbed 30-fold with its emergence into new countries, and it has also expanded from urban to rural areas in the last decade [1]. This rate is still increasing despite vector control efforts and the widespread use of clinical guidelines. According to World Health Organisation (WHO), an estimated 390 million dengue infections are occurring every year, in which Asian countries account for 70% of the total cases [2]. A primary intervention and prevention plan is essential to evade the predicted prevalence of dengue, as this will impose a huge burden on the country's people and its economy. According to WHO, if the disease cases are sensitively detected in the early stages of an epidemic, emergency space spraying and intensified larviciding can benefit reduction measures [1].

The biosensors in this aspect are vital because of their remote sensing ability and portability. Biological investigations can be carried out using portable sensors with the help of microelectrodes and conventional electrodes [3]. Various biosensors used in detecting tuberculosis, hCG (pregnancy), HIV, cancer, glucose, and malaria are either based on optical or electrochemical methods [4]. However, apart from being accurate and providing high precision, these sensors also suffer from some limitations. Some of these sensors require purification of the samples, and some methods are based on laboratory investigations [3]. The rising interest in microwave biosensors has grown to a new level that they will be potentially made available in the commercial market very soon. This is certainly because high-frequency

waves can pass through the cell membrane and interact with the cytoplasm, eventually interacting with γ -dispersion [4].

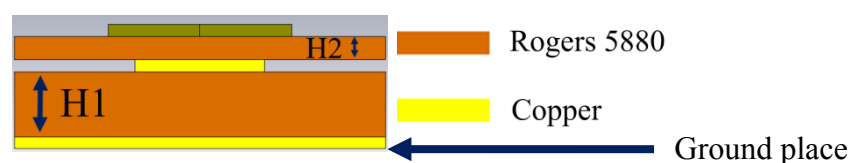
In these developments, the metamaterial is considered an exceptionally suitable candidate due to its extraordinary properties. This is due to the highly concentrated fields provided by metamaterial structures that enhance sensitivity [5]. Split Ring Resonator (SRR) and its complementary version are the two most researched configurations of metamaterials [6]. Metamaterial exhibits negative permittivity, permeability, and refractive index values at different microwave frequency ranges, which is not possible in commonly available materials. Subwavelength resonators in biosensing are used to achieve a significant response against small variations in electrical properties of the surroundings through the resonant frequency shift [7]. Every material exhibits certain electrical characteristics due to its tangent loss, permittivity, and permeability, which can be characterised by biosensors.

Numerous studies have been conducted on the blood's dielectric properties. Recent works have focused on the permittivity of the blood for investigations on glucose concentration [8]–[11]. A biosensor should be small to accommodate the various applications in the medical field [12]. To the best knowledge of the author, a metamaterial sensor operating at millimetre-wave frequencies has not been proposed to date. The majority of sensing elements proposed are found to be operating at low microwave frequencies, which are larger than $50 \times 50 \text{ cm}^2$, and their sensitivity is relatively low. These concerns highlight the need for an alternative sensor design that is simple to use, highly sensitive, and small in size. Furthermore, sensitivity increases at millimetre-wave frequencies because this band provides greater dielectric changes in the blood than low microwave frequencies [13]. Several techniques for sample investigations have been carried out using metamaterial-based resonators. The model with an engraved space in the substrate was proposed in [14], [15] comprising of a metamaterial liquid sensor integrating feed transmission line (FTL). However, this concept of engraved space to hold

material under test (MUT) may potentially produce errors in repeated measurements. Since the substrate is etched to control blood samples on the sensor's surface, it is difficult to clean the area entirely after every measurement. The unwanted blood particles of the previous measurement can interfere with the outcomes. Resultantly, the design needs replacement after few measurements. Therefore, the sensor design based on double layers is proposed with a replaceable top layer suitable for repeated measurements. In this way, a highly sensitive metamaterial-based resonator sensor operating at millimetre wave frequencies can be constructed to detect dengue using a small quantity of blood sample. The double-layered designed sensor has been validated through experiments. In addition, the potential of the sensor in integration with the IoMT systems is also discussed in this paper.

2. Design

As the name implies, the double-layered structure is made up of two sheets of the Rogers RT/Duroid 5880, a low dielectric loss substrate with a dielectric constant (ϵ_r) of 2.2 and a loss tangent ($\tan\delta$) of 0.004. Fig. 1(a) shows a side view of the proposed design containing two substrate layers (H1 and H2). Simultaneously, copper with a thickness of 0.035 mm is acting as the conducting element. The top substrate layer (H2) has no ground while the top substrate layer (H1) has a full ground plane on the bottom side. A metamaterial resonating structure with a dimension of $20 \times 10 \text{ mm}^2$ and a thickness of 0.127 mm is printed on the top substrate layer is depicted in Fig. 1(b). The bottom layer, with an overall dimension of $20 \times 30 \times 1.57 \text{ mm}^3$ as shown in Fig. 1(c) contains the FTL linked to the ports. The integrated proposed design for the sensor is depicted in Fig. 1(d). As can be seen, the top layer is to be magnetically coupled to the bottom layer. The optimised parameters for the sensor are given in Table 1.



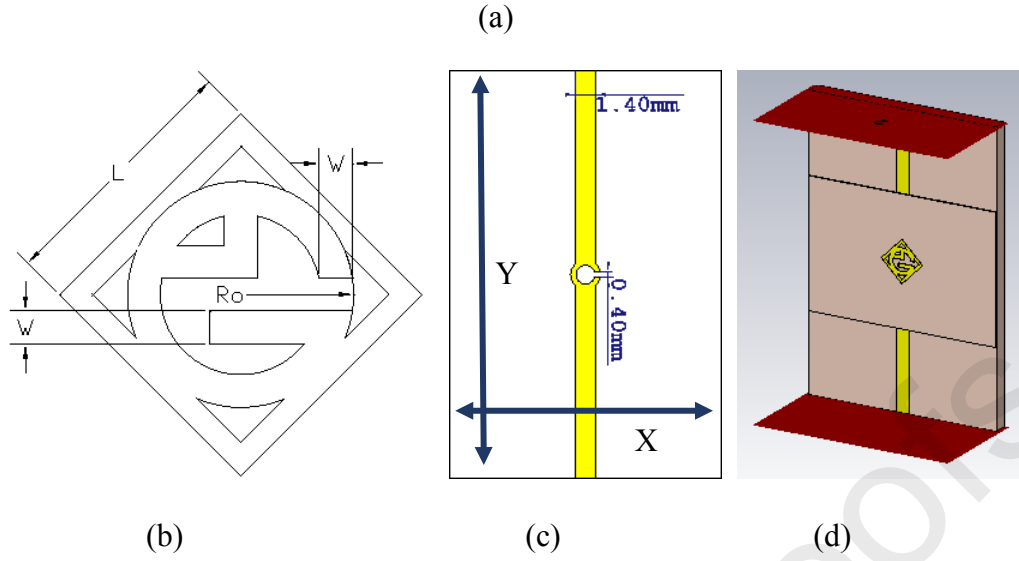


Figure 1. Resonator (a) side view (b) metamaterial structure on top layer (c) transmission line on the bottom layer and (d) perspective view of integrated design.

Table 1. Key parameters of design and their values.

R_0 (mm)	L (mm)	W (mm)	X (mm)	Y (mm)	H1 (mm)	H2 (mm)
1.1	3.1	0.4	20	30	1.57	0.127

The circular opening loop in the bottom layer can work as a magnetic dipole, which produces an oscillating magnetic field perpendicular to the top substrate layer [16]. Two layers of the resonators under the magnetic field excitation will induce currents in a similar direction, eventually forming positive mutual inductance (M). At the same time, the flow of induced currents is resisted by the opening of the ring at the bottom layer, due to which clockwise and counter-clockwise rotation of charges appear on the bottom and top substrate layer, respectively. Fig. 2 represents the mechanism of the magnetic field creating the surface current distributions for structures on both layers, while Fig. 3 shows the resulting surface current distributions on top and bottom layers. The directions of the charges in two layers are opposite due to the opening of two layers (ring at the bottom and G-shape at top) in the same direction that generates coupling capacitance (C_c). The mutual inductance (M) and coupling capacitance (C_c) both offer a significantly improved overall inductance and capacitance, which also contribute to the resonant frequency as of Equation (1). The highest electric field intensity

observed on the main square patch, which amounts to around 11 kV/m as shown in Fig. 4. A higher electric field is observed at the outer part of the resonator because of the coupling between the shape on the bottom layer and the resonator on the top layer.

$$F_r = \frac{1}{2\pi\sqrt{LC}} \quad (1)$$

Where C represents the equivalent capacitance of the structure, while L represents the overall inductance.

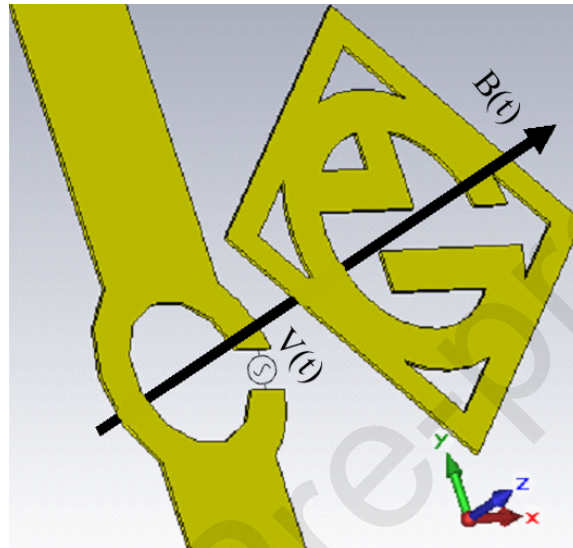


Figure 2. The magnetic excitation caused by feeding.

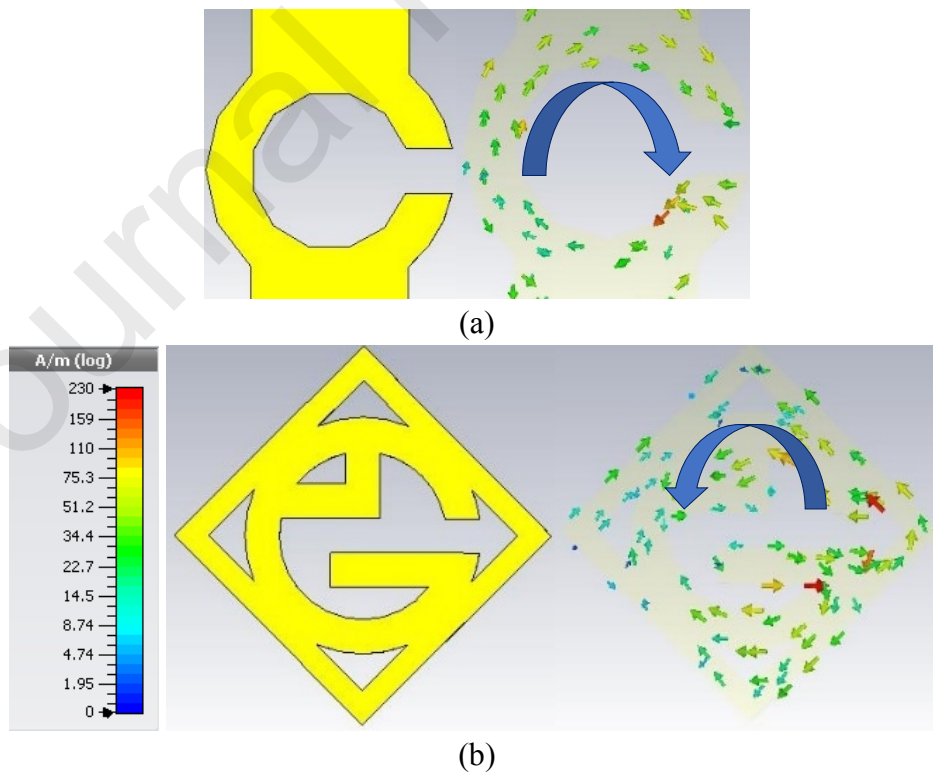


Figure 3. Surface current distributions for (a) bottom layer and (c) top layer.

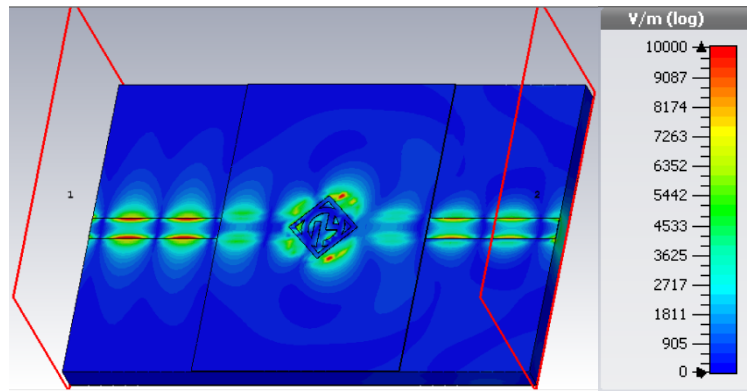


Figure 4: Electric field intensity for integrated structure

The metamaterial structure was modelled and simulated using the Finite Integration Technique (FIT) in CST Microwave Studio. The sensing process was analysed by simulating the blood's dielectric characteristics on the sensor. Later, a blood sample was introduced in simulation onto the surface of a top layer covering all resonators' areas, as shown in Fig. 5. Blood's dispersive characteristics were modelled in the 20-40 GHz range by employing the values of the blood's permittivity and loss tangent calculated by Gabriel [17].

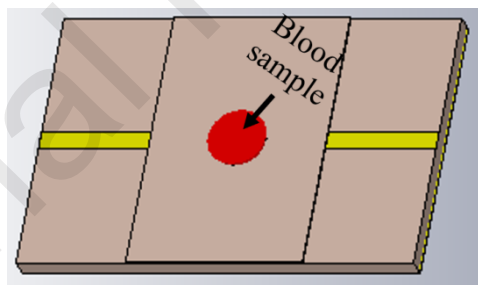


Figure 5. Placement of blood sample on the front layer of a double-layered sensor.

Since the millimetre-wave frequencies are sensitive to the dielectric changes, the resonant frequency is observed after the placement of MUT. Fig. 6 shows the reflection coefficient (S_{11}) and transmission coefficient (S_{21}) of the designed sensor for the integrated structure. The sensor observes two resonant frequencies in the reflection coefficient. The first highest negative peak of the S_{11} is generated at 26.76 GHz with an amplitude of -35.3 dB and the second resonant frequency is 34.34 GHz with an amplitude of -20.7 dB. The resonance in

transmission coefficient (S_{21}) is seen around 38 GHz above our desired range. The first resonance (S_{11}) without blood at 26.76 GHz happens to be the primary resonant frequency as its sharpness in resonance is better than that of the resonance at 34.34 GHz.

It can be noticed from Fig. 6 that the resonant frequency (S_{11}) after placement of the sample has a higher depth in amplitude than resonance without MUT. The reflection coefficient for the sensor shows resonances at 27.22 GHz, and the highest negative peak is observed at a negative amplitude of 44.32 dB. On the other hand, the transmission coefficient is flat after the placement of the blood sample on the sensor's surface. Therefore, only S_{11} is considered in further analysis for blood sensing following previously published works [8], [18].

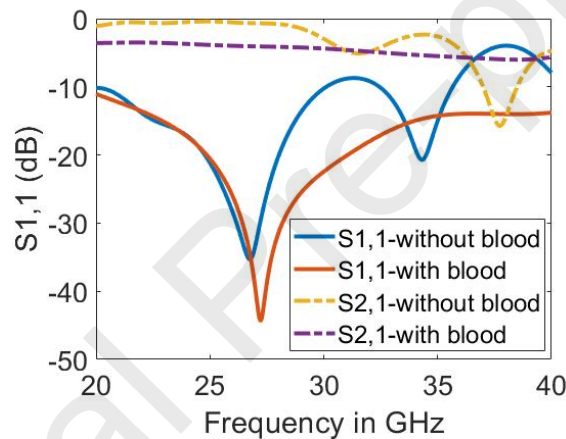


Figure 6. The resonant frequency with and without blood sample on sensor's surface.

3. Parametric Study

Because of the energy exchange between the ring at the bottom layer and the resonator at the top layer, the excitation in the feeding system is very robust. The feeding systems are typically coplanar waveguide and microstrip lines. In this type of feeding mechanism, microwave network matching must be optimised so that microwave energy can be magnetically linked to the metamaterial structure at the top layer. As a result, the essential factors indicated in Table 1 were modified to investigate their impact on resonance. The radius of the split-ring (R_0) of the construction shown in Figure 1b was adjusted from 0.9 mm to 1.2 mm. It was discovered that this parameter has a strong influence on the resonant frequency. As illustrated in Figure 7, a 0.1 mm change in this parameter shifts the resonant frequency from 33 GHz to 28 GHz. This parameter appears to have a significant impact on the design's performance. The value of the variable square length (L) parameter from Figure 1b was modified from 3 mm to 3.3 mm in simulations. The square length was found to have the opposite influence on the resonant frequency as the radius (R_0). As shown in Figure 8, increasing this parameter shifts the resonance frequency to the right. The length of the square, in addition to the radius, has a

significant impact on the resonance frequency. It is because increasing the length will lead the square to get disconnected from the G-shape when its size exceeds the radius of the G-shape. When the line width (W) of the entire structure is varied, as shown in Figure 1b (a), the amplitude of the reflection coefficient changes, but no apparent resonance shift is observed. The amplitude of the reflection coefficient was increased by increasing the linewidth from 0.25 mm to 0.45 mm, as illustrated in Figure 9. In comparison to the length and radius, the linewidth appears to have little effect on the resonance. This, however, alters the sharpness of the resonant frequency.

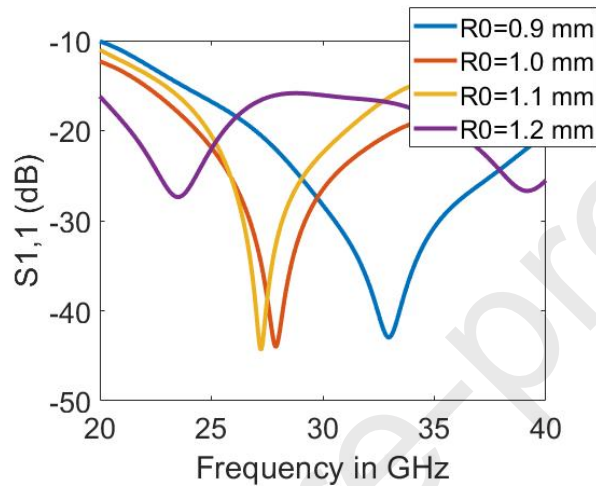


Figure 7. Resonant frequency on different values of “ R_0 ” in sensor.

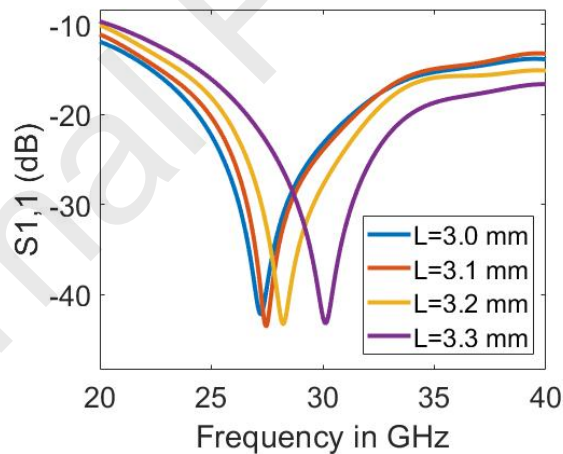


Figure 8. Resonant frequency on different values of “ L ” in sensor.

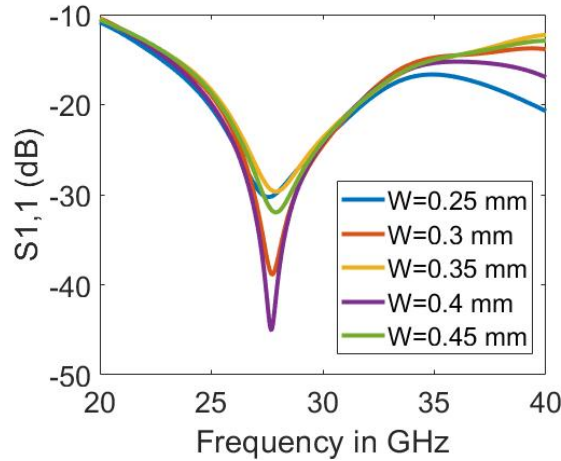


Figure 9. Resonant frequency on different values of “W” in sensor.

4. Perturbation in Reflection Coefficient

The performance of the proposed sensor was estimated by varying the blood’s permittivity level. According to clinical practice guidelines for dengue infection management in adults, dengue investigation necessitates testing of two major factors: platelet count and haematocrit ratio [19]. A study on blood coagulometry, which happens due to low platelet counts, found a direct correlation of blood coagulation with permittivity [20]. In contrast, the conductivity decreased with the increase in haematocrit levels in another study [21]. It should be recalled that permittivity at high frequencies takes a complex form as of Equation (2):

$$\varepsilon_r = \varepsilon_r' + \varepsilon_r'' \quad (2)$$

where ε_r is the complex permittivity of any dielectric material and ε_r' is a real part of permittivity, while ε_r'' is an imaginary part of permittivity. According to Equation (3), the imaginary part of permittivity can be written in the form of conductivity.

$$\varepsilon_r'' = \frac{\sigma}{\omega \varepsilon_0} \quad (3)$$

Thus, both of those parameters (real and imaginary parts of blood's permittivity) exhibit a decrease when blood is coagulated and/or haematocrit levels are increased. In addition, a recent study conducted on haemoglobin levels also revealed that the real and imaginary parts of permittivity are increased when haemoglobin levels reduce [22]. This indicates that the

permittivity must reduce when haemoglobin levels are increased due to dengue infections [23]. In sum, as much as the platelet counts decrease or the haematocrit ratio increase in blood, the blood permittivity reduces correspondingly. Therefore, to draw the blood's dielectric behaviour in dengue, the real and imaginary parts of the complex permittivity of blood have been reduced from their normal levels.

In response to the variation in the dielectric constant and the tangent loss, the reflection coefficient (S_{11}) changes were obtained due to the added capacitance of MUT. Fig. 10 shows the reflection coefficient behaviour of the sensor on varying blood's permittivity. The resonant frequencies are shifted towards higher frequencies in the sensor for proportions of blood samples with reduced real and imaginary permittivity. This shift is in agreement with the outcomes provided by simulations and measurements carried out in other works with the variation in blood's permittivity [7], [24]–[26]. The resonance at 27.22 GHz shows normal platelet counts and haematocrit levels, whereas the resonance shifting towards higher frequencies shows the tendency of infection in the blood, i.e., higher the resonant frequency, the increasing levels of a severe case. The colour gradient bar shows the boundary between healthy people (blue) and infected people (red).

Using the resonant frequencies of the perturbation phenomenon, we used regression analysis to calculate the intensity of infection. As shown in Fig. 11, the equation obtained in regression analysis, which has the determination coefficient (R^2) of 0.9729 can help determine the infection's intensity level, with 0 being the normal level and 8 representing the highly severe case.

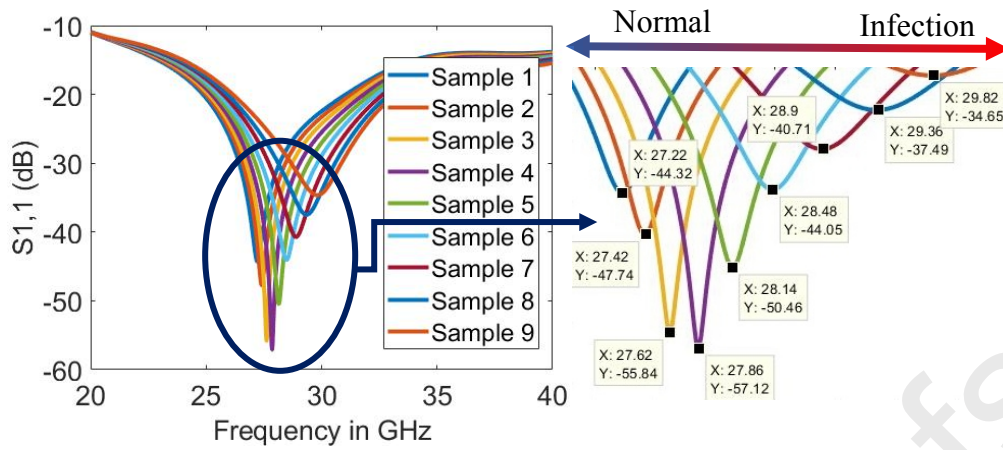


Figure 10. Perturbation under different blood samples on sensor.

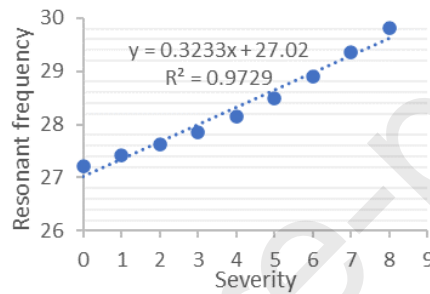


Figure 11. Severity analysis of dengue infections.

5. Measurement and Verification of Results

The measurements were taken at the Campus Pagoh, Universiti Tun Hussein Onn Malaysia. The reflection coefficient was measured using N5234B PNA-L Microwave Vector Network Analyzer (VNA). A 2.40 mm reusable SMA connector was used to connect the VNA with the microstrip lines of the resonator. Before measurement, the VNA was calibrated using 85056A Calibration Kit to remove any systematic error.

The fabricated sensor is depicted in Fig. 12. The 2.4 mm reusable SMA connector was used as RF ports connecting the design to VNA. Fig. 13 shows the simulated and measured results of the integrated sensor. It is authenticated that the simulated and measured results are in good agreement. However, slight variations in amplitude can occur due to environmental parameters, imperfect fabrication, and interferences.



Figure 12. Fabricated design of sensor.

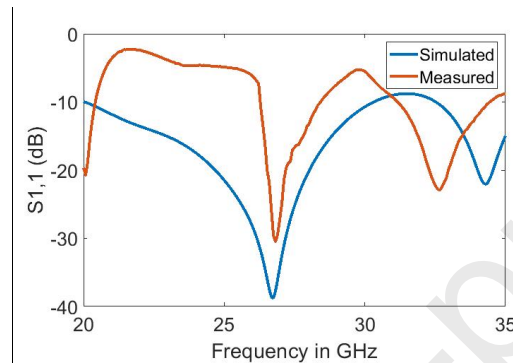


Figure 13. Simulated and measured reflection coefficient of the sensor without sample.

It is well known that one of the significant constituents of biological materials is water [27]. For instance, the contents of the water in erythrocytes range from 55% to 75%. Similarly, biomolecules are held in a fluidic medium in biological suspensions; thus, the large proportion of suspension is governed by water. Human organs, tissues and blood also contain water as a dominant component [17]. The response of electromagnetic waves in a microwave with water is thus, used as a foundation for developing microwave biosensors [28]. In the experimental setup, samples were made up of 'Tap Water', 'Methylated Spirit with 90% Alcohol' and 'Methylated Spirit with 75% Alcohol'.

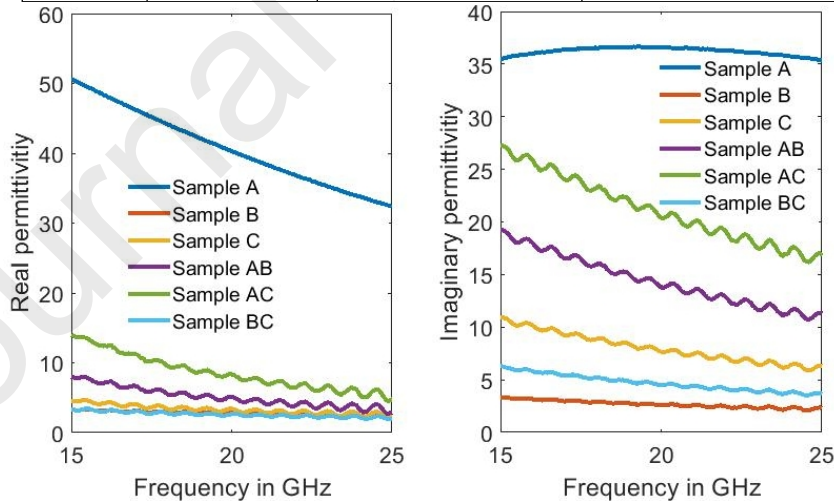
It is broadly studied that the permittivity of alcohol is lower than the permittivity of water [29], [30]. This same phenomenon was observed in the 20-35 GHz range when the permittivity of the samples was measured during experiments. Consequently, mixing alcohol in water can reduce the permittivity of the water, which happens to the blood's permittivity when the dengue virus infects it. Therefore, the water-alcohol mixtures were used as an alternate

sample to replicate the dielectric behaviour of blood and its behaviour in dengue infection. The composition of each sample tested during experiments is listed in Table 2.

Later, the permittivity of each sample modelled was determined using the "Keysight 85070E Dielectric Probe Kit". It was reaffirmed that the permittivity of liquid reduces with the increasing concentration of alcohol. The real and imaginary parts of permittivity for the samples listed in Table 2 are depicted in Fig. 14. The permittivity of liquid reduces with the increasing concentration of alcohol. In this way, the infected blood's dielectric characteristics can be correlated with the alcohol contents in water. The measured reflection coefficient (S_{11}) of the samples, when inserted on the sensor's surface, are demonstrated in Fig. 15.

Table 2. Composition of liquid samples.

Sample code	Vol. of Tap Water	Vol. of 90% Methylated Spirit	Vol. of 75% Methylated Spirit
A	50	-	-
B	-	50	-
C	-	-	50
AB	25	25	-
AC	25	-	25
BC	-	25	25



(a)

(b)

Figure 14. Measured (a) real and (b) imaginary permittivity of liquid samples.

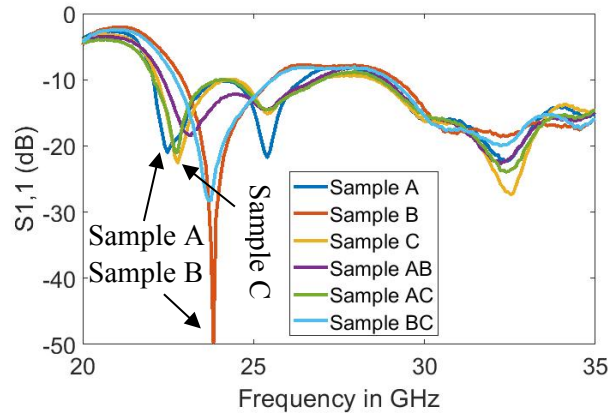


Figure 15. Measured reflection coefficients for liquid samples on the sensor.

Sample A is considered pure water or non-infected sample in which the addition of alcohol contents reduces its permittivity. Samples with reduced permittivity can be described as infected or abnormal blood samples. It can be realised that the highest shift to the lower frequencies of resonance is obtained in the case of water. This is because the permittivity of water is higher than the permittivity of alcohol [30]. On the other hand, Sample B observed the highest shift to the higher frequencies due to the highest alcohol contents, which has relatively low permittivity. These results indicate that if Sample B is the response of infected blood, its resonance moves towards higher frequencies. This follows the trend of simulated results where the reflection coefficient moves to the right with decreasing blood's permittivity, as shown in Fig. 10.

6. Discussion

In the previous sections, the metamaterial-based design of the sensor is proposed for detecting the dengue virus. The design consists of a replaceable top layer on which the blood sample is inserted for testing. Thus, the measurements can be carried out without disconnecting the bottom layers i.e., feed transmission line from the VNA. Based on this, we calculate the sensor's sensitivity and compare it with the state-of-art metamaterial-based sensors presented

in previous works for blood-sensing applications. Later, we propose the broader prospective implementation of the presented sensor in detecting dengue infections remotely using IoMT technology.

7.1. Sensitivity Analysis

Different metamaterial sensors have been presented for various blood sensing applications, which vary with each other in terms of operating frequency, size, sensing parameter, coefficient of determination (R^2) and sensitivity. The basic function of sensitivity in the metamaterial-based millimetre-wave sensor is to obtain a shift in the resonant frequency with the variation in the dielectric permittivity of blood. The sensor was optimised to have electromagnetic fields (H_0 and E_0) at equilibrium in place of a blood sample with normal dielectric characteristics. When the feed transmission line is excited by the electric fields, metamaterial structure with inductive patches cause resonance. When the dielectric characteristics of the blood change, the metamaterial structure's capacitance changes, which produce new electromagnetic fields (H_1 and E_1). These newly generated electromagnetic fields cause the shifting in the resonant frequency of the structure, which is mathematically represented as Equation (4) [31]:

$$\frac{\Delta f_r}{f_r} = \frac{\int_v (\Delta \epsilon E_1 E_0 + \Delta \mu H_1 H_0) dv}{\int_v (\epsilon_0 |E_0|^2 + \mu_0 |H_0|^2) dv} \quad (4)$$

According to Equation (4), blood's permittivity, permeability cause the perturbation in resonance. The sensor's sensitivity based on the perturbation phenomenon can be determined by calculating the ratio of a shift in resonance and the permittivity variation of the blood sample. This ratio is mathematically represented in Equation (5).

$$S = \lim_{\Delta(\epsilon_h - \epsilon_n) \rightarrow 0} \frac{\Delta f_s - \Delta f_r}{\Delta \epsilon_s - \Delta \epsilon_r} \quad (5)$$

where f_r is the resonant frequency at reference sample, while f_s represent the resonant frequency reduced permittivity. The highest change in the blood's dielectric constant is represented by ϵ_s , whereas the normal blood permittivity is represented by ϵ_r .

The sensor's sensitivity is calculated using Equation (5). The significant factors in calculating sensitivity are the shift in the resonance and the change in the sample's permittivity levels. It is clear from the sensitivity that the sensor can detect enhanced sensitivity when there is a decrease in permittivity due to dengue infection. As the permittivity of the blood is reduced, the sensitivity is found to be increasing. A comparison between the presented sensor and other metamaterial-based blood sensors is presented in Table 3. Based on this table, different sensors have different average sensitivity, which is mainly because of the design and the operating frequency.

Table 3. Comparison of state of the art metamaterial-based sensors for blood sensing

Ref.	Operating frequency (GHz)	Sensing technique	Determination coefficient (R^2)	Sensitivity (GHz)	Size (mm^2)
[32]	1-5	S_{21}	0.9902	0.026	50×20
[25]	2.4-2.6	S_{11}	0.995	0.005	9×9
[33]	5.5-8.5	S_{21}	N/A	0.035	30×18
[34]	8.0-8.4	S_{11}	N/A	0.025	40×30
[35]	2.0-2.75	S_{21}	N/A	0.0185	80×100
[36]	15.5 – 17.0	S_{11}	N/A	0.025	30×35
This work	27.5-30	S_{11}	0.9729	0.325	20×30

Compared with previously studied sensors in blood sensing applications, our sensor has the better resonant shift per unit dielectric change, which is 0.325 GHz on average, according to Equation (5). In addition to sensitivity, the coefficient of determination is another parameter that determines how the regression model predicts the data. This parameter, which ranges from 0 to 1, is also known as the square of the correlation coefficients. The closer the value is to 1, the better the model fits. This study yielded an R^2 value of 0.9729, indicating that 97.29 % of predictability in the shift in resonance was accounted for using a linear regression model, while 2.71 % went unaccounted for.

7.2. *Potential Integration in IoMT System*

The world has witnessed the advent of the Internet of Medical Things (IoMT) in the medical field, which presents a convergence of humans, data, and devices. The remote sensing capability has triggered further expansion in this field due to the connection of conventional sensors with the web. These devices in sensing technology integrated with wireless connectivity can help in detecting the dengue outbreak. This study is a preliminary step in the development of the system shown in Fig. 16. This system can be established using layers: sensing, interface, network, and service, as illustrated in [37] for the application of meat-quality monitoring. The developed sensor needs to be connected with the microwave analyzer through a coaxial transmission line, which needs to be connected with a Bluetooth adapter. In this way, the subject can test the blood and send the data directly from the sensor to remotely control the IoMT device. The analyzer not only excites the sensor's feed transmission electromagnetically but also reads the output signal. This signal can be read by the single-chip radio with a USB host. The analyzer needs to be configured to transfer the measured signal to the gateway through a Bluetooth network. This process can be carried out instantaneously or testing data can be saved and sent later based on the network availability. IoMT in this system is defined as the system consisting of the metamaterial-based sensor for detecting the dengue virus so that data can be collected, exchanged, and acted upon with or without human intervention.

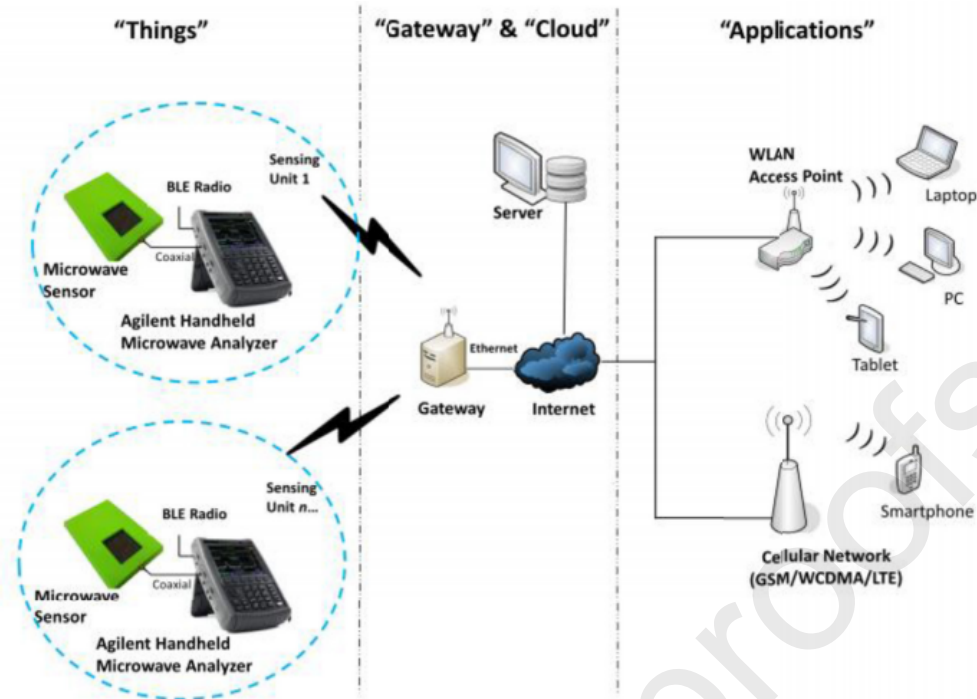


Figure 16. Layout of IoMT-based dengue detection system [37]

7. Conclusion

In this paper, a double-layered metamaterial-based resonator has been proposed for the detection of the dengue virus. The sensor detects the changes in the blood's permittivity due to the influencing parameters of dengue infection. Two key challenges were mainly addressed; first, multiple tests can be conducted with the replaceable top layer without removing the transmission layer connected to VNA. Second, the proposed sensor will be helpful in the early detection of the outbreak. Additionally, the sensor can be operated non-invasively as it requires a small quantity of blood around 0.05 ml, which can be extracted using the finger-prick technique. Experimental results obtained demonstrated good sensitivity of the designs for dielectric characterisation of the samples. Furthermore, the sensor's integration with the IoMT system is discussed, which is still in the early stages of development for a practical application. The proposed research work's prototype implementation demonstrates the feasibility of

developing a sensor for COVID-19 that can detect the virus quickly and efficiently and keep track of red zones with a high number of cases.

Funding Statement

This study is funded by the Ministry of Higher Education (MoHE) Malaysia under Fundamental Research Grant Scheme Vot No. FRGS/1/2019/TK04/UTHM/02/13, and it is partially sponsored by Universiti Tun Hussein Onn Malaysia (UTHM).

References

- [1] World Health Organization, “Dengue guidelines for diagnosis, treatment, prevention and control,” *World Heal. Organ.*, 2009.
- [2] “Dengue Fever: Statistics and Key Facts,” 2020. <https://www.prudential.com.my/en/we-do-pulse/all-stories/dengue-fever-statistics-and-key-facts/> (accessed Jul. 07, 2021).
- [3] S. RoyChoudhury, V. Rawat, A. H. Jalal, S. N. Kale, and S. Bhansali, “Recent advances in metamaterial split-ring-resonator circuits as biosensors and therapeutic agents,” *Biosens. Bioelectron.*, vol. 86, pp. 595–608, Dec. 2016, doi: 10.1016/j.bios.2016.07.020.
- [4] P. Mehrotra, B. Chatterjee, and S. Sen, “EM-wave biosensors: A review of RF, microwave, mm-wave and optical sensing,” *Sensors (Switzerland)*, vol. 19, no. 5, p. 1013, Feb. 2019, doi: 10.3390/s19051013.
- [5] A. Ebrahimi, J. Scott, and K. Ghorbani, “Differential sensors using microstrip lines loaded with two split-ring resonators,” *IEEE Sens. J.*, vol. 18, no. 14, pp. 5786–5793, Jul. 2018, doi: 10.1109/JSEN.2018.2840691.
- [6] A. Salim and S. Lim, “Review of recent metamaterial microfluidic sensors,” *Sensors (Switzerland)*, vol. 18, no. 1, p. 232, Jan. 2018, doi: 10.3390/s18010232.
- [7] Y. I. Abdulkarim *et al.*, “Novel Metamaterials-Based Hypersensitized Liquid Sensor

- Integrating Omega-Shaped Resonator with Microstrip Transmission Line,” *Sensors*, vol. 20, no. 3, p. 943, Feb. 2020, doi: 10.3390/s20030943.
- [8] A. Kandwal *et al.*, “Highly Sensitive Closed Loop Enclosed Split Ring Biosensor With High Field Confinement for Aqueous and Blood-Glucose Measurements,” *Sci. Rep.*, vol. 10, no. 1, p. 4081, Dec. 2020, doi: 10.1038/s41598-020-60806-9.
- [9] M. N. Hasan, S. Tamanna, P. Singh, M. D. Nadeem, and M. Rudramuni, “Cylindrical Dielectric Resonator Antenna Sensor for Non-Invasive Glucose Sensing Application,” in *2019 6th International Conference on Signal Processing and Integrated Networks, SPIN 2019*, Mar. 2019, pp. 961–964, doi: 10.1109/SPIN.2019.8711633.
- [10] H. Choi *et al.*, “Design and In Vitro Interference Test of Microwave Noninvasive Blood Glucose Monitoring Sensor,” *IEEE Trans. Microw. Theory Tech.*, vol. 63, no. 10, pp. 3016–3025, Oct. 2015, doi: 10.1109/TMTT.2015.2472019.
- [11] S. Kim *et al.*, “Noninvasive in vitro measurement of pig-blood d-glucose by using a microwave cavity sensor,” *Diabetes Res. Clin. Pract.*, vol. 96, no. 3, pp. 379–384, Jun. 2012, doi: 10.1016/j.diabres.2012.01.018.
- [12] L. La Spada, F. Bilotti, and L. Vegni, “Metamaterial biosensor for cancer detection,” in *Proceedings of IEEE Sensors*, Oct. 2011, pp. 627–630, doi: 10.1109/ICSENS.2011.6127103.
- [13] A. E. Omer, S. Safavi-Naeini, R. Hughson, and G. Shaker, “Blood Glucose Level Monitoring Using an FMCW Millimeter-Wave Radar Sensor,” *Remote Sens.*, vol. 12, no. 3, p. 385, Jan. 2020, doi: 10.3390/rs12030385.
- [14] A. Tamer *et al.*, “Metamaterial based sensor integrating transmission line for detection of branded and unbranded diesel fuel,” *Chem. Phys. Lett.*, vol. 742, p. 137169, Mar. 2020, doi: 10.1016/j.cplett.2020.137169.
- [15] Ş. Dalgaç *et al.*, “Grease oil humidity sensor by using metamaterial,” *J. Electromagn.*

- Waves Appl.*, vol. 34, no. 18, pp. 2488–2498, Dec. 2020, doi: 10.1080/09205071.2020.1824690.
- [16] Y.-D. Wang *et al.*, “Design of Double-Layer Electrically Extremely Small-Size Displacement Sensor,” *Sensors*, vol. 21, no. 14, p. 4923, Jul. 2021, doi: 10.3390/s21144923.
- [17] S. Gabriel, R. W. Lau, and C. Gabriel, “Physics in Medicine & Biology. The dielectric properties of biological tissues: III. Parametric models for the dielectric spectrum of tissues,” *Phys. Med. Biol.*, vol. 41, no. 11, pp. 2271–2293, Nov. 1996, doi: 10.1088/0031-9155/41/11/003.
- [18] J. A. Byford, K. Y. Park, and P. Chahal, “Metamaterial inspired periodic structure used for microfluidic sensing,” in *Proceedings - Electronic Components and Technology Conference*, 2015, vol. 2015-July, pp. 1997–2002, doi: 10.1109/ECTC.2015.7159876.
- [19] M. H. T. A. S. (MaHTAS), “CPG Management of Dengue Infection In Adults (Third Edition),” 2015. [Online]. Available: https://medic.usm.my/anaest/images/Malaysia_CPG_Dengue_Infection_2015.pdf.
- [20] K. Igari, T. Kudo, T. Toyofuku, and Y. Inoue, “The use of dielectric blood coagulometry in the evaluation of coagulability in patients with peripheral arterial disease,” *BMC Clin. Pathol.*, 2017, doi: 10.1186/s12907-017-0054-z.
- [21] F. Jaspard, M. Nadi, and A. Rouane, “Dielectric properties of blood: An investigation of haematocrit dependence,” *Physiol. Meas.*, 2003, doi: 10.1088/0967-3334/24/1/310.
- [22] A. Santorelli *et al.*, “Investigation of Anemia and the Dielectric Properties of Human Blood at Microwave Frequencies,” *IEEE Access*, 2018, doi: 10.1109/ACCESS.2018.2873447.
- [23] N. K. Tripathi, A. Shrivastava, P. K. Dash, and A. M. Jana, “Detection of Dengue Virus,” in *Methods in molecular biology (Clifton, N.J.)*, vol. 665, Methods Mol Biol, 2010, pp.

51–64.

- [24] S. Mohammadi, A. V. Nadaraja, K. Luckasavitch, M. C. Jain, D. June Roberts, and M. H. Zarifi, “A Label-Free, Non-Intrusive, and Rapid Monitoring of Bacterial Growth on Solid Medium Using Microwave Biosensor,” *IEEE Trans. Biomed. Circuits Syst.*, vol. 14, no. 1, pp. 2–11, Feb. 2020, doi: 10.1109/TBCAS.2019.2952841.
- [25] A. Ebrahimi, J. Scott, and K. Ghorbani, “Microwave reflective biosensor for glucose level detection in aqueous solutions,” *Sensors Actuators A Phys.*, vol. 301, p. 111662, Jan. 2020, doi: 10.1016/j.sna.2019.111662.
- [26] Y. I. Abdulkarim *et al.*, “The Detection of Chemical Materials with a Metamaterial-Based Sensor Incorporating Oval Wing Resonators,” *Electronics*, vol. 9, no. 5, p. 825, May 2020, doi: 10.3390/electronics9050825.
- [27] K. Kageyama, Y. Onoyama, H. Kogawa, E. Goto, and K. Tanabe, “The maximum and minimum water content and cell volume of human erythrocytes in vitro,” *Biophys. Chem.*, vol. 34, no. 1, pp. 79–82, Sep. 1989, doi: 10.1016/0301-4622(89)80044-4.
- [28] S. Guha, F. I. Jamal, and C. Wenger, “A Review on Passive and Integrated Near-Field Microwave Biosensors,” *Biosensors*, vol. 7, no. 4, p. 42, Sep. 2017, doi: 10.3390/bios7040042.
- [29] Z. O. Rodríguez-Moré, H. Lobato-Morales, R. A. Chávez-Pérez, and J. L. Medina-Monroy, “Complex dielectric permittivity of rum and its mixtures with methanol, ethanol, and water at frequencies up to 15 GHz,” *J. Microw. Power Electromagn. Energy*, vol. 52, no. 1, pp. 16–30, Jan. 2018, doi: 10.1080/08327823.2017.1421013.
- [30] R. Augustine, S. Raman, and A. Rydberg, “Relative permittivity measurements of Et–OH and Mt–OH mixtures for calibration standards in 1–15 GHz range,” *Electron. Lett.*, vol. 50, no. 5, pp. 358–359, Feb. 2014, doi: 10.1049/el.2013.4300.
- [31] A. Armghan, T. M. Alanazi, A. Altaf, and T. Haq, “Characterization of Dielectric

- Substrates Using Dual Band Microwave Sensor,” *IEEE Access*, vol. 9, pp. 62779–62787, 2021, doi: 10.1109/ACCESS.2021.3075246.
- [32] G. Govind and M. J. Akhtar, “Metamaterial-Inspired Microwave Microfluidic Sensor for Glucose Monitoring in Aqueous Solutions,” *IEEE Sens. J.*, vol. 19, no. 24, pp. 11900–11907, Dec. 2019, doi: 10.1109/JSEN.2019.2938853.
- [33] S. Kiani, P. Rezaei, and M. Fakhr, “Dual-Frequency Microwave Resonant Sensor to Detect Noninvasive Glucose-Level Changes Through the Fingertip,” *IEEE Trans. Instrum. Meas.*, vol. 70, pp. 1–8, 2021, doi: 10.1109/TIM.2021.3052011.
- [34] A. Verma, S. Bhushan, P. N. Tripathi, M. Goswami, and B. R. Singh, “A defected ground split ring resonator for an ultra-fast, selective sensing of glucose content in blood plasma,” *J. Electromagn. Waves Appl.*, vol. 31, no. 10, pp. 1049–1061, 2017, doi: 10.1080/09205071.2017.1325011.
- [35] G. Govind and M. J. Akhtar, “Design of an ELC resonator-based reusable RF microfluidic sensor for blood glucose estimation,” *Sci. Rep.*, vol. 10, no. 1, p. 18842, Dec. 2020, doi: 10.1038/s41598-020-75716-z.
- [36] M. U. Memon and S. Lim, “Millimeter-wave chemical sensor using substrate-integrated-waveguide cavity,” *Sensors (Switzerland)*, vol. 16, no. 11, 2016, doi: 10.3390/s16111829.
- [37] M. T. Jilani, M. Z. U. Rehman, A. M. Khan, O. Chughtai, M. A. Abbas, and M. T. Khan, “An implementation of IoT-based microwave sensing system for the evaluation of tissues moisture,” *Microelectronics J.*, vol. 88, pp. 117–127, Jun. 2019, doi: 10.1016/j.mejo.2018.03.006.

Declaration of interests

The authors declare that they have no known competing financial interests or personal relationships that could have appeared to influence the work reported in this paper.